Acta Crystallographica Section D
Biological Crystallography
ISSN 0907-4449

Expression, crystallization and phasing of vacuolar H$^+$-ATPase subunit C (Vma5p) of *Saccharomyces cerevisiae*

Omri Drory, Adi Mor, Felix Frolow* and Nathan Nelson

Department of Biochemistry, The George S. Wise Faculty of Life Sciences, Tel Aviv University, Tel Aviv 69978, Israel

Correspondence e-mail: felixf@tauex.tau.ac.il

Received 24 June 2004
Accepted 9 August 2004

The expression, crystallization and phasing of subunit C (Vma5p) of the yeast (*Saccharomyces cerevisiae*) vacuolar proton-translocating ATPase (V-ATPase) is described. The expressed protein consists of 412 residues: 392 from the reading frame of Vma5p and 20 N-terminal residues originating from the plasmid. Diffraction-quality crystals were obtained using the hanging-drop and sitting-drop vapour-diffusion methods assisted by streak-seeding, with PEG 3350 as precipitant. The crystals formed in hanging drops diffracted to 1.80 Å and belong to space group $P4_32_12_1$, with unit-cell parameters $a = b = 62.54$, $c = 327.37$ Å, $\alpha = \beta = \gamma = 90^\circ$. The structure was solved using SIRAS with a $Lu(O_2C_2H_3)_2$ heavy-atom derivative.

1. Introduction

Vacuolar H$^+$-ATPase (V-ATPase) is present in almost every eukaryotic cell and energizes several internal organelles and other membrane assemblies (Nelson & Harvey, 1999). It produces proton motive force by hydrolysing ATP. The energy provided by V-ATPase facilitates the acidification of intracellular compartments in eukaryotic cells and plays an important role in receptor-mediated endocytosis, intracellular traffic processes and protein degradation (Nishi & Forgac, 2002; Nelson *et al.*, 2002). V-ATPase is a multisubunit enzyme consisting of two distinct functional domains V_1 and V_0. The V_0 domain is composed of five different integral membrane subunits with a total molecular weight of 260 kDa. The 570 kDa V_1 domain consists of eight subunits (Nelson & Harvey, 1999). The V_1 domain, much like the F_1 domain in F-type ATPases, is responsible for ATPase catalytic activity, whereas the V_0 domain is involved in the translocation of protons across the membrane. Unlike the F-type ATPases, little is known about the atomic architecture of the V-type ATPases or how the proton translocation is coupled to ATP hydrolysis. Determination of the structure of the ATP-generating domain of the bovine F-type ATPase provided the first atomic details of how the F_1 domain is assembled and binds nucleotides (Abrahams *et al.*, 1994; Leslie & Walker, 2000). The structure supported the proposal that ATP synthesis is catalyzed in a rotary catalytic fashion (Abrahams *et al.*, 1994; Boyer, 1997). Even though the α- and β-subunits of the F-type ATPases exhibit sequence homology to the Vma2p and Vma1p subunits of the V-ATPases and the rotary motion of catalysis is presumed to be similar among these enzymes, the molecular architecture of the V-ATPases appears to be more complex (Aviezer-Hagai *et al.*, 2003). The number of known subunits of the V-type ATPases exceeds that of the F-type ATPases (Perzov *et al.*, 2001). Also, recent evidence from electron microscopy suggests that the overall structure and shape of the two enzymes may be considerably different (Zhang *et al.*, 2003; Wieczorek *et al.*, 2003).

Several genes that code for various subunits in the V_1 domain as well as the V_0 domain of the ATPase from yeast have been identified and characterized (Nelson & Harvey, 1999). Subunit C was first cloned from bovine adrenal medulla by obtaining amino-acid sequences from the purified subunit of the bovine adrenal medullae enzyme (Nelson *et al.*, 1990). Subsequently, the gene VMA5 encoding this subunit in yeast was cloned and interrupted (Beltran *et al.*, 1992), resulting in the typical V-ATPase null phenotype (Nelson & Nelson, 1990). Vma5p was found to be necessary for the assembly of complete V-ATPase (Beltran *et al.*, 1992; Ho, Hill *et al.*, 1993; Ho, Hirata *et al.*, 1993) but not for its V_1 part (Doherty & Kane, 1993). The two proteins from bovine preparations and yeast are 37% identical and, like all other V_1 subunits, subunit C is released from the membrane by cold inactivation (Beltran *et al.*, 1992). Subunit C exhibits no homology to any of the F-ATPase subunits and consequently its function and distribution in the four functional parts of the enzyme are not known. Recently, it has been shown that subunit C of tobacco hawkmoth (*Manduca sexta*) V-ATPase is capable of actin binding, suggesting a role in coordinating the traffic of membranes containing V-ATPase (Vitavska *et al.*, 2003). Subunit C has been shown to be essential for catalysis and V_1–V_0 assembly but not for the

assembly of the V_1 subcomplex (Ho, Hill *et al.*, 1993).

Outstanding electron-microscopy work demonstrating the general structure of V-ATPase has been performed (Wilkens *et al.*, 2004). So far, out of all the eukaryotic V-ATPase subunits only the high-resolution structure of subunit H is known (Sagermann *et al.*, 2001). Here, we report the successful crystallization of the VMA5 gene product (also identified as subunit C) of the yeast vacuolar proton ATPase. The amino-acid sequence consists of 412 residues, 20 of which at the N-terminus originate from the plasmid.

2. Materials and methods

2.1. Cloning, expression, purification, crystallization and heavy-atom derivative preparation

The VMA5 gene from *Saccharomyces cerevisiae* was amplified by PCR using the primers TAT CAT ATG GCT ACT GCG TTA TAT ACT GC (sense) and TAT CTC GAG TTA TAA ATT GAT TAT ATA CAT CAC AAA T (antisense) containing *Nde*I and *Xho*I, respectively. The PCR product was extracted from gel, digested by *Nde*I and *Xho*I and subcloned into the respective restriction sites of a pET28a(+) expression vector (Novagen). The expressed protein contained a six-His tag at its C-terminus. The plasmid was transformed into C43 and C41 cells (based on BL21 cells; courtesy of Professor J. E. Walker) and selected on 25 µg ml^{-1} kanamycin-containing Luria–Bertani (LB) agar plates. Positive clones were identified by analytical PCR and by DNA sequencing.

For expression, selected clones were grown in 9 l TB medium containing kanamycin to mid-log phase and subsequently induced with 0.65 m*M* isopropyl-β-D-thiogalactopyranoside for about 2 h at a temperature of 310 K. Cells were harvested by centrifugation at 3000*g* for 10 min. The pellet was resuspended in 180 ml of 0.3 *M* sucrose, 20 m*M* MOPS pH 7.0 buffer. After addition of DNAaseI and 1 m*M* PMSF, the cells were ruptured using a French press. The homogenate was then subjected to centrifugation at 10 000*g* for 10 min. The supernatant was ultracentrifugated at 150 000*g* for 35 min and the supernatant was collected.

NaCl was added to the supernatant to a concentration of 200 m*M* and it was passed through a 100 ml DEAE-cellulose column (Whatman). The flowthrough was applied onto a 2 × 10 cm nickel–NTA affinity column (Qiagen). The column was washed with 40 ml of a solution containing 20 m*M* imidazole, 250 m*M* NaCl and 25 m*M* Tris pH 8.0 and eluted with a solution containing 300 m*M* imidazole, 250 m*M* NaCl and 25 m*M* Tris pH 7.0. The protein was further purified using a MonoQ ion-exchange column (Bio-Rad) in an FPLC system (Bio-Rad). The protein was concentrated using a second nickel-affinity column and then dialyzed overnight against crystallization buffer (30 m*M* Tris pH 7.2 and 50 m*M* NaCl) and concentrated to 1 ml (∼50 mg ml^{-1}) using a Vivaspin 20 ml concentrator (Vivascience). The purity of the protein was analyzed by SDS–PAGE. Typically, a 9 l preparation yielded approximately 50 mg purified protein.

Crystallization conditions were screened at 289 and 277 K using pre-formulated crystal screen solutions using commercially available kits (Hampton Research, Laguna Hills, California, USA) employing the hanging-drop vapour-diffusion method. Initially, diffraction-quality crystals were obtained after around four months in a hanging drop containing 20%(*v*/*v*) PEG 3350, 0.2 *M* disodium tartrate pH 7.2 (PEG/Ion screen, condition No. 36). These crystals were used for streak-seeding of freshly prepared hanging drops. The reservoir contained 0.5 ml of the same solution. Tetragonal crystals of bipyramidal non-polar morphology (Fig. 1*a*) appeared in 24 h and grew to dimensions of about 0.6 × 0.3 × 0.3 mm in one week. Sitting drops using the same crystallization solution produced crystals of rhombohedral morphology in addition to the tetragonal crystalline form.

Crystals were cryoprotected by successive soaking in cryobuffer [25%(*v*/*v*) ethylene glycol, 20%(*v*/*v*) PEG 3350, 0.2 *M* disodium tartrate]. For heavy-atom derivatives the crystals were soaked for 1–3 h in cryobuffer containing 5–25 m*M* heavy atom. Heavy-atom compounds were selected from commercially available kits (Hampton Research, Laguna Hills, California, USA) on the basis of their pH being suitable for solubility in the cryobuffer.

2.2. X-ray data collection and processing

Data from two native and 20 putative heavy-atom derivative crystals were collected using synchrotron radiation (ID14-EH2 and ID29 beamline stations at ESRF, Grenoble, France). Cryoprotected crystals were mounted in a cryoloop (Teng, 1990) and flash-cooled to 100 K using an Oxford Cryosystem (Cosier & Glazer, 1986). All data sets were collected using ASDC detectors at ESRF beamlines ID14-2 and ID29 at wavelengths of 0.934 and 0.9756 Å, respectively. The tetragonal crystals belong to the tetragonal space group $P4_12_12$ (or $P4_32_12$), with unit-cell parameters $a = b = 62.54$, $c = 327.37$ Å, $\alpha = \beta = \gamma = 90^\circ$. Native crystal data were collected to 1.80 Å and derivative data to 2.0 Å resolution. Data were integrated, scaled and merged using the *HKL* program package (Otwinowski & Minor, 1997).

The unit-cell parameters of the rhombohedral crystals were $a = b = 192.3$, $c = 34.2$ Å, $\alpha = \beta = 90$, $\gamma = 120^\circ$ (hexagonal setting) and the space group is $R3$ based on a data set collected using in-house X-ray facilities with an R-AXIS IV image-plate detector and Cu $K\alpha$ radiation.

The presence of only one monomer in the asymmetric unit for both the tetragonal and rhombohedral forms (corresponding to solvent contents of 64.9 and 68.5%, respec-

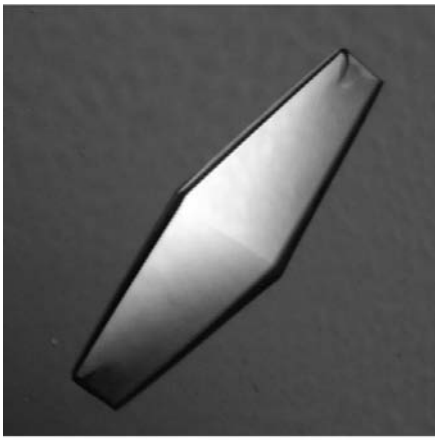

(*a*)

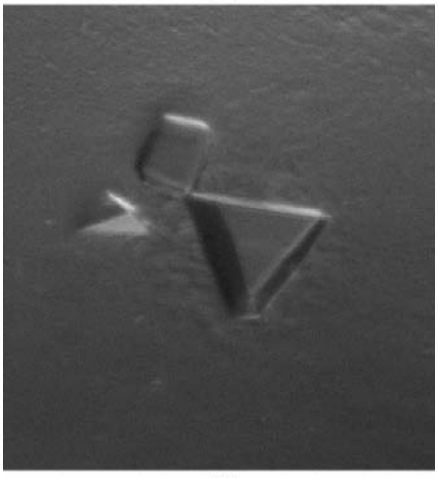

(*b*)

Figure 1
Crystals of Vma5p from *S. cerevisiae*. (*a*) Typical tetragonal crystals, grown in a hanging drop; the longest dimension is ∼0.6 mm. (*b*) Typical rhombohedral form, grown in sitting drops; the largest crystals are approximately 0.3 mm in the longest dimension.

tively) was supported by calculated Matthews coefficients of 3.5 and 3.9 Å^3 Da^{-1}, respectively (Matthews, 1968) and self-rotation functions calculated by *POLARRFN* (Collaborative Computational Project, Number 4, 1994) that showed no significant peaks.

2.3. Phasing

Initial inspection of diffraction data collected from tetragonal crystals of the native and heavy-atom derivative crystals revealed a high degree of isomorphism between the native and derivative crystals (data not shown). However, only a heavy-atom derivative based on $Lu(O_2C_2H_3)_2$ revealed a Patterson function map with significant and consistent Harker peaks for both isomorphous and anomalous signals (Fig. 2). The positions of heavy atoms were determined using data between 46 and 2.0 Å resolution by manual interpretation of the Patterson function with the aid of *RSPS* (Collaborative Computational Project, Number 4, 1994; Knight, 2000) and confirmed by automatic procedures implemented in *SOLVE* (Terwilliger & Berendzen, 1999). Ambiguity in the space-group selection ($P4_12_12$ *versus* $P4_32_12$) was resolved by *SOLVE*, yielding a set of phases based on anomalous and isomorphous differences with FOM = 0.27, which was improved to FOM = 0.78 during the phase-modification procedure in *RESOLVE* (Terwilliger & Berendzen, 1999). Partial main chain automatically traced by *RESOLVE* was used as an input to *ARP*/*wARP* (Perrakis *et al.*, 1999) and the complete structure was traced and its sequence assigned in a single *ARP*/*wARP* run. After *ARP*/*wARP*, minor corrections to the structure were made using methods implemented in program *O* (Jones *et al.*, 1991).

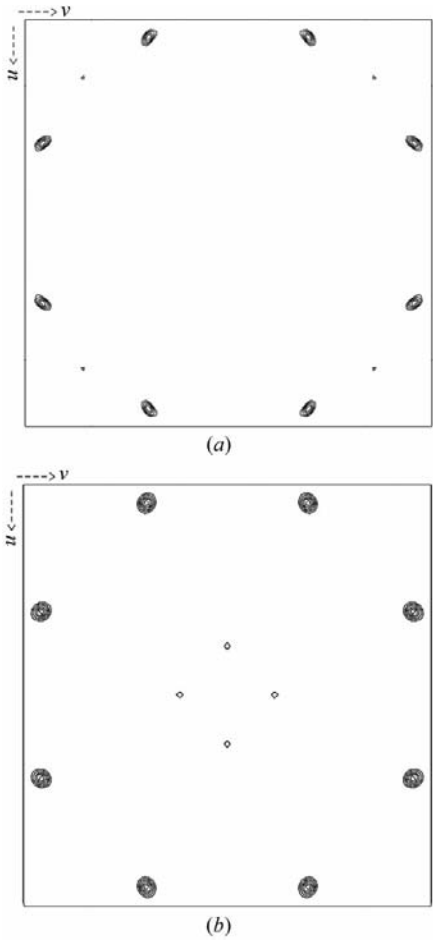

Figure 2
Harker sections (w = 1/4) of Patterson maps calculated in the 46.0–2.0 Å resolution range. (*a*) Isomorphous difference Patterson map between native and derivative data; contours are drawn at the 0.5σ level starting from 3σ. (*b*) Anomalous difference Patterson map for lutetium acetate derivative data; contours are drawn at the 2σ level starting from 6σ.

Table 1
Data-collection and processing statistics.

Values in parentheses are for the highest resolution shell.

	Native	$Lu(O_2C_2H_3)_2$
Experimental conditions		
X-ray source	ESRF (ID14-EH2 station)	ESRF (ID29 station)
Wavelength (Å)	0.933	0.9756
Temperature (K)	100	100
Detector	ADSC	ADSC
Crystal parameters		
Space group	$P4_32_12$	$P4_32_12$
Unit-cell parameters		
a (Å)	62.54	62.67
b (Å)	62.54	62.67
c (Å)	337.37	335.68
$\alpha = \beta = \gamma$ (°)	90	90
Resolution (Å)	20–1.80 (1.83–1.80)	20–2.06 (2.10–2.06)
Mosaicity (°)	0.123	0.437
Matthews coefficient (Å^3 Da^{-1})	3.7	3.7
Solvent content (%)	66.8	66.8
Asymmetric unit (monomers)	1	1
Data processing		
No. observed reflections	370231	490156
No. unique reflections	63954	43077
Completeness (%)	98.7 (99.9)	99.5 (100)
R_{sym}†	0.077 (0.577)	0.085 (0.265)
$\langle I/\sigma(I)\rangle$	23.9 (2.5)	23.3 (11.42)
Phasing procedure		
FOM based on heavy atom	0.27 (0.19)	
Phasing power based on heavy atom	0.68 (0.78)	
FOM after phase modification	0.78 (0.58)	

† $R_{sym} = \sum|I - \langle I\rangle|/\sum I$.

3. Discussion

Implementation of the streak-seeding method significantly improved crystal quality and expedited the crystallization, which otherwise took several months for crystal to appear. Only one crystalline form was produced in the hanging-drop experiments, whereas in the sitting-drop setup rhombohedral crystals were produced in addition to the tetragonal crystal form. This finding may be significant, as different crystalline forms may have different crystal packing contacts, perhaps stabilizing regions of the molecule that may be disordered in the other crystalline forms. The absence of a suitable model for molecular replacement based on a sequence-similarity search among all known structures led us to consider the MIR method and several heavy-atom derivatives were prepared. Heavy-atom soaking experiments in accordance with the crystallization buffer pH to improve solubility and/or stability of heavy-atom compounds proved to be a significant factor in obtaining a high-quality heavy-atom derivative. The native and Lu heavy-atom derivative crystals appeared to be highly isomorphous, diffracted to similar level of resolution and possessed solvent contents of about 65%, thus facilitating phasing and phase-modification procedures (Table 1). The structure was solved by a combination of SIRAS and partial structure-evolution methods. Refinement of the vacuolar H$^+$-ATPase subunit C (Vma5p) structure from *S. cerevisiae* is now in progress.

We gratefully acknowledge the ESRF for synchrotron beam time and staff scientists of the ID14-2 and ID29 stations for their

assistance. OD acknowledges Tel Aviv University for a PhD student scholarship.

References

Abrahams, J. P., Leslie, A. G. W., Lutter, R. & Walker, J. E. (1994). *Nature (London)*, **370**, 621–628.

Aviezer-Hagai, K., Padler-Karavani, V. & Nelson, N. (2003). *J. Exp. Biol.* **206**, 3227–3237.

Beltran, C., Kopecky, J., Pan, Y. C. E., Nelson, H. & Nelson, N. (1992). *J. Biol. Chem.* **267**, 774–779.

Boyer, P. D. (1997). *Annu. Rev. Biochem.* **66**, 717–749.

Collaborative Computational Project, Number 4 (1994). *Acta Cryst.* D**50**, 760–763.

Cosier, J. & Glazer, A. M. (1986). *J. Appl. Cryst.* **19**, 105–107.

Doherty, R. D. & Kane, P. M. (1993). *J. Biol. Chem.* **268**, 16845–16851.

Ho, M. N., Hill, K. J., Lindorfer, M. A. & Stevens, T. H. (1993). *J. Biol. Chem.* **268**, 221–227.

Ho, M. N., Hirata, R., Umemoto, N., Ohya, Y., Takatsuki, A., Stevens, T. H. & Anraku, Y. (1993). *J. Biol. Chem.* **268**, 18286–18292.

Jones, T. A., Zou, J. Y., Cowan, S. W. & Kjeldgaard, M. (1991). *Acta Cryst.* A**47**, 110–119.

Knight, S. D. (2000). *Acta Cryst.* D**56**, 42–47.

Leslie, A. G. W. & Walker, J. E. (2000). *Philos. Trans. R. Soc. London, Ser. B*, **355**, 465–471.

Matthews, B. W. (1968). *J. Mol. Biol.* **33**, 491–497.

Nelson, H., Mandiyan, S., Noumi, T., Moriyama, Y., Miedel, M. C. & Nelson, N. (1990). *J. Biol. Chem.* **265**, 20390–20393.

Nelson, H. & Nelson, N. (1990). *Proc. Natl Acad. Sci. USA*, **87**, 3503–3507.

Nelson, N. & Harvey, W. R. (1999). *Physiol. Rev.* **79**, 361–385.

Nelson, N., Sacher, A. & Nelson, H. (2002). *Nature Rev. Mol. Cell Biol.* **3**, 876–881.

Nishi, T. & Forgac, M. (2002). *Nature Rev. Mol. Cell Biol.* **3**, 94–103.

Otwinowski, Z. & Minor, W. (1997). *Methods Enzymol.* **276**, 307–326.

Perrakis, A., Morris, R. & Lamzin, V. S. (1999). *Nature Struct. Biol.* **6**, 458–463.

Perzov, N., Padler-Karavani, V., Nelson, H. & Nelson, N. (2001). *FEBS Lett.* **504**, 223–228.

Sagermann, M., Stevens, T. H. & Matthews, B. W. (2001). *Proc. Natl. Acad. Sci. USA*, **98**, 7134–7139.

Teng, T.-Y. (1990). *J. Appl. Cryst.* **23**, 387–391.

Terwilliger, T. C. & Berendzen, J. (1999). *Acta Cryst.* D**55**, 849–861.

Vitavska, O., Wieczorek, H. & Merzendorfer, H. (2003). *J. Biol. Chem.* **278**, 18499–18505.

Wieczorek, H., Huss, M., Merzendorfer, H., Reineke, S., Vitavska, O. & Zeiske, W. (2003). *J. Bioenerg. Biomembr.* **35**, 359–366.

Wilkens, S., Takao, I. & Forgac, M. (2004). In the press.

Zhang, H. M., Kurisu, G., Smith, J. L. & Cramer, W. A. (2003). *Proc. Natl Acad. Sci. USA*, **100**, 5160–5163.